HHS Public Access

Author manuscript

Otol Neurotol. Author manuscript; available in PMC 2016 October 01.

Published in final edited form as:

Otol Neurotol. 2015 October ; 36(9): 1554–1561. doi:10.1097/MAO.0000000000000838.

Cochlear Implant Electrode Effect on Sound Energy Transfer within the Cochlea during Acoustic Stimulation

Nathaniel T. Greene, PhD[a,b,*], **Jameson K. Mattingly, MD**[a], **Herman A. Jenkins, MD**[a], **Daniel J. Tollin, PhD**[a,b], **James R. Easter, MS, PE**[c], and **Stephen P. Cass, MD, MPH**[a]

[a]Department of Otolaryngology, University of Colorado School of Medicine, Aurora, CO

[b]Department of Physiology and Biophysics, University of Colorado School of Medicine, Aurora, CO

[c]Cochlear Boulder LLC, Boulder, CO

Abstract

Hypothesis—Cochlear implants (CI) designed for hearing preservation will not alter mechanical properties of the middle and inner ear as measured by intracochlear pressure (P_{IC}) and stapes velocity (V_{stap}).

Background—CIs designed to provide combined electrical and acoustic stimulation (EAS) are now available. To maintain functional acoustic hearing, it is important to know if a CI electrode can alter middle or inner ear mechanics, as any alteration could contribute to elevated low-frequency thresholds in EAS patients.

Methods—Seven human cadaveric temporal bones were prepared, and pure-tone stimuli from 120Hz–10kHz were presented at a range of intensities up to 110 dB SPL. P_{IC} in the scala vestibuli (P_{SV}) and tympani (P_{ST}) were measured with fiber-optic pressure sensors concurrently with V_{Stap} using laser Doppler vibrometry. Five CI electrodes from two different manufacturers, with varying dimensions were inserted via a round window approach at six different depths (16–25 mm).

Results—The responses of P_{IC} and V_{Stap} to acoustic stimulation were assessed as a function of stimulus frequency, normalized to SPL in the external auditory canal (EAC), in baseline and electrode inserted conditions. Responses measured with electrodes inserted were generally within ~5 dB of baseline, indicating little effect of cochlear implant electrode insertion on P_{IC} and V_{Stap}. Overall, mean differences across conditions were small for all responses, and no substantial differences were consistently visible across electrode types.

Conclusions—Results suggest that the influence of a CI electrode on middle and inner ear mechanics is minimal, despite variation in electrode lengths and configurations.

[*]Nathaniel T. Greene, Department of Physiology and Biophysics, University of Colorado School of Medicine, 12800 E. 19th Ave., Rm 7401G, Aurora, CO 80045, United States, Tele: 303-724-0637, Fax: 303-724-1961, nathaniel.greene@ucdenver.edu.

Conflict of Interest Statement:

Stephen P. Cass is a consultant on the Surgical Advisory Board for Cochlear Corporation.
James R. Easter is an employee at Cochlear Boulder LLC.

Keywords

Cochlear implant; electroacoustic stimulation; intracochlear pressures; hearing preservation

Introduction

Direct electrical stimulation of the cochlea via cochlear implantation has successfully treated moderate to severe hearing deficits for several decades (1). Recently, attention has been given to cochlear implant (CI) use by patients with severe to profound high frequency hearing loss, and significant residual low frequency hearing. This simultaneous electrical and acoustic stimulation (EAS) allows access to acoustically useful low frequency hearing that can lead to benefits in music appreciation and sound localization, while providing access to high frequency information useful for speech perception, especially in noise (2–4).

In order to achieve the benefits of combined electrical and acoustic stimulation, sufficient hearing must be preserved for acoustic stimulation following cochlear implantation. However, in a subset of patients functional residual hearing is lost following CI implantation or shortly thereafter (5). As a result, CI manufacturers have developed shorter, thinner, and softer electrodes, and surgeons have refined surgical techniques to emphasize preservation of residual hearing (6–8). Nevertheless, many patients still lose functional residual hearing immediately or some time after CI implantation.

Multiple etiologies have been suggested for loss of residual hearing, including direct trauma to intracochlear structures and/or inflammation and cell death related to the electrode (9). Additionally, there may be alterations of inner ear mechanics or cochlear impedance resulting in conductive hearing loss (10–14). Multiple mechanisms have been suggested to underlie such a conductive loss, including changes in middle ear (e.g. effusion) or inner ear mechanics, damage to intracochlear structures (e.g. basilar membrane, osseous spiral lamina, spiral ligament), change in perilymph volume, alteration of round window (RW) compliance, and host reactions to the electrode (e.g. fibrosis, osteoneogenesis) (10,11,14–17). Studies evaluating these etiologies, specifically alteration of middle and inner ear mechanics, have been contradictory regarding the biomechanical influence of a CI electrode (15–22). Regardless, any degree of hearing loss is of concern as it can affect the residual low frequency hearing thresholds that are necessary to gain benefit from EAS stimulation.

To explore the effect of a CI electrode on middle and inner ear mechanics, we combine laser Doppler vibrometry (LDV) of stapes velocity (V_{Stap}) and differential intracochlear sound pressure (P_{IC}) measurements. These methods are well suited for this study, as P_{IC} offers the most direct quantification of mechanical input to the cochlea, and further allow comparisons of the effects of various CI electrodes on this signal (23–25).

Materials and Methods

Seven ears in five fresh-frozen whole or hemicephalic heads, with intact temporal bones and no history of middle ear disease were evaluated (Lone Tree Medical, Littleton, CO, USA). The use of cadaveric human tissue was in compliance with the University of Colorado

Anschutz Medical Campus Institutional Biosafety Committee (COMIRB EXEMPT #14-1464). Responses were assessed in whole-head specimens immediately following tests studying the mechanisms of bone-conducted hearing (26,27) that in some cases followed stimulation patterns used previously in the lab (28).

Temporal Bone Preparation

Temporal bone preparation and experimental procedures were similar to methods described previously by our laboratory (29–31), as well as other authors (23), modified accommodate for the preparation and experimental time required for using whole head specimens. Preparation and experimentation were typically completed on separate days, thus in order to minimize degradation to the tissue, the following schedule was followed for hemi-cephalic/whole head specimens. First, specimens were thawed and temporal bones were prepared in one or both ears and refrozen within approximately 12 or 24 hours. Second, specimens were rethawed; one ear was tested within approximately 12 hours in hemicephalic, and both ears were tested during the course of two consecutive days (~48 h) in whole heads. The total duration that each specimen was left at room temperature was < ~24 hours for hemi-cephalic, and < 72 hours in whole head specimens.

Temporal bones were prepared using the following procedure: specimens were thawed in warm water, and the external ear canal and tympanic membrane were inspected for damage. A canal-wall-up mastoidectomy and extended facial recess approach was performed to visualize the incus, stapes, and round window (30). The cochlear promontory near the oval and round windows was thinned with a small diamond burr in preparation for pressure sensor insertion into the scala vestibuli (SV) and scala tympani (ST).

Cochleostomies into the ST and SV were created under a droplet of water using a fine pick. Pressure sensors (FOP-M260-ENCAP, FISO Inc., Quebec, QC, Canada), were inserted into the SV and ST using rigidly mounted micromanipulators (David Kopf Instruments, Trujunga, CA). Pressure sensor diameter is approximately 310 μm (comprised of a 260 μm glass tube covered in polyimide tubing with ~25 μm wall thickness), and are inserted into the cochleostomy until the sensor tip is just within the bony wall of the cochlea (~100 μm). Cochleostomies were made as small as possible, such that the pressure probes fit snuggly within, but inserted completely into the opening. Pressure sensor sensitivity is rated at ± 1 psi (6895 Pa). The signal is initially processed by a signal conditioner (Veloce 50; FISO Inc., Quebec, QC, Canada), which specifies the precision and resolution of at 0.3% and 0.1% of full scale, or ~20.7 Pa and 6.9 Pa respectively. Sensors were sealed within the cochleostomies with alginate dental impression material (Jeltrate; Dentsply International Inc., York, PA). Location of the cochlostomies with respect to the basilar membrane were verified visually after each experiment by removing the bone between the two cochleostomies.

Out-of-plane velocity of V_{Stap} was measured with a single-axis LDV (OFV-534 & OFV-5000; Polytec Inc., Irvine, CA) mounted to a dissecting microscope (Carl Zeiss AG, Oberkochen, Germany). Microscopic retro-reflective glass beads (Polytec Inc., Irvine, CA) were placed on the neck and posterior crus of the stapes to ensure a strong LDV signal since the stapes footplate was typically obscured by the presence of the stapes tendon. In all LDV

measurements, the position of the laser was held as constant as possible between experimental conditions (32,33).

CI electrodes used in these experiments were: Nucleus Hybrid L24 (HL24; Cochlear Ltd, Sydney, Australia), Nucleus CI422 Slim Straight inserted at 20 and 25 mm (SS20 & SS25; Cochlear Ltd, Sydney, Australia), Nucleus CI24RE Contour Advance (NCA; Cochlear Ltd, Sydney, Australia), HiFocus Mid-Scala (MS; Advanced Bionics AG, Stäfa, Switzerland), and HiFocus 1j (1J; Advanced Bionics AG, Stäfa, Switzerland). Electrode dimensions are provided in Table 1. Electrodes were inserted sequentially, under water, into the ST via a RW approach. Electrodes were typically inserted in order of smallest to largest (i.e. the order listed above) in an attempt to minimize the effects of damage caused by insertion on subsequent recordings. Potential effects of insertion order are expected to be minimal, owing to the similarity in responses across conditions (see Results), and the lack of any observable effect in one experiment in which the electrode insertion order was shuffled. The cochleostomy was sealed following each electrode insertion with alginate dental impression material, and excess water was removed via suction from the middle ear cavity.

Stimuli Presentation and Data Acquisition

All experiments were performed in a double-walled sound-attenuating chamber (IAC Inc., Bronx, NY). Stimuli were generated digitally, presented to the specimen closed-field magnetic speaker (MF1; Tucker-Davis Technologies Inc., Alachua, FL) powered by one channel of a stereo amplifier (SA1), and driven by an external sound card (Hammerfall Multiface II, RME, Haimhausen, Germany) modified to eliminate high-pass filtering on the analog output. Stimuli were generated and responses recorded at 44100 Hz, and controlled by a custom-built program in MATLAB (MathWorks Inc., Natick, MA). Sounds were delivered to the ear canal through a custom-made foam and rigid rubber insert earplug inserted into a speculum, secured in the ear canal with cyanoacrylate adhesive, and sealed with Jeltrate. The sound intensity in the ear canal was measured with a probe-tube microphone (type 4182; Brüel & Kjær, Nærum, Denmark) and signal conditioner (B&K type 2690). The microphone probe tube was inserted through a small hole in the rubber tubing, and placement near the tympanic membrane was verified by visual inspection through the tubing prior to earplug insertion. Stimuli were twenty short tone pips (twenty cycles at each frequency) presented two frequencies per octave between 120 and 10240 Hz. Stimuli were presented for at least five repetitions each at 10V amplitude. Input from the microphone, LDV, and pressure sensors were simultaneously captured via the sound card analog inputs.

Data Analysis

The responses measured were chosen in order to assess the input to the inner ear as a function of the acoustic input in order to assess features of the transmission pathway. Thus, responses are shown as transfer functions, i.e. measured velocity (V_{Stap}) and pressures (P_{SV} & P_{ST}) are presented normalized to SPL in the EAC (P_{EC}). Resulting transfer functions (H_{Stap}, H_{SV}, & H_{ST}) were calculated from the FFT of the response to pure tone stimulation in accordance with the conventions of ASTM F2504 (34). The magnitude of the LDV signal was adjusted using a correction factor ($1/\cos\theta$) based on a visual estimate of the difference

in angle between the primary axis of the stapes (i.e. a vector normal to the stapes footplate and running through the head of the stapes) and the orientation of the LDV laser (θ; usually ~45°). All acquired signals were band-pass filtered between 15 Hz and 15 kHz with a second order Butterworth filter for data analysis. The noise floor for transfer function recordings are shown on plots by calculating the transfer function magnitude for each recording on a 200 ms recording immediately *preceding* each stimulus presentation, normalizing the sound pressure level recorded in the ear canal *during* the stimulus presentation, and are shown in figures as gray dots. Responses shown are calculated from the average of five repetitions, and data points shown include only those points with a signal-to-noise ratio of greater than 3 dB and with a noise floor below either the upper bound of the 95% confidence interval (95% CI) or mean ± standard deviation of responses reported previously in the literature (gray bands; 23,35). Additionally, signal strength is indicated in individual transfer function plots by symbol size (small, > 3 dB; medium, > 6 dB; large, > 9 dB signal to noise ratio).

Results

Acoustic closed-field transfer functions

Responses were assessed prior to making the RW cochleostomy in order to verify the condition of the specimen, and to establish baseline responses. Baseline measurements were repeated after CI electrode insertion conditions in two early experiments in order to ensure that the specimen condition had not changed over the course of the experiment, but this procedure was deemed unnecessary and was not completed in most experiments. Baseline closed-field acoustic transfer function magnitudes (H_{Stap}, H_{SV}, and H_{ST}) for 6 specimens that met inclusion criteria are shown in Figure 1A. Responses were overlayed onto the 95% confidence interval for H_{Stap}, and the mean ± standard deviation of responses observed for H_{SV} and H_{ST} reported previously (23,35). Several specimens showed frequencies that lie outside of these bands in one or more response; however these deviations are relatively small, thus may be expected based upon normal physiological variability, and should not affect the results since all analyses are relative to baseline measurements (29,30,36). Transfer function phase was likewise calculated, and baseline responses are shown superimposed on normal responses observed in the literature (23,35) in Figure 1B. Response phases show unwrapping errors at high frequencies, owing to the relatively sparse frequency sampling used in this study, but were largely consistent with those prior reports.

Effect of CI electrode insertion on measured responses

Immediately following baseline measurements, transfer function recordings were repeated with the CI electrodes described above. Figure 2A demonstrates an example set of responses in one representative specimen (249L). Baseline transfer functions are represented by circles, while transfer functions recorded with CI electrodes inserted are shown with their respective gray shade and symbol. In general, there is a great deal of overlap across transfer function recordings, suggesting that none of the electrodes substantially affected the responses recorded.

Figure 2B shows the differences in transfer function magnitudes recorded with cochlear implant electrodes inserted compared to the baseline for the same specimen as in Figure 2A. Responses are shown in units of dB difference from baseline as a function of stimulus frequency. Difference curves calculated from H_{Stap} and H_{SV} generally fall within ±5 dB (except responses recorded with MS, which showed a magnitude decrease of ~ 10dB), indicating that transfer functions recorded with the CI electrodes inserted were comparable to baseline. Similarly, H_{ST} difference functions show responses within ±5 dB at frequencies above 1 kHz, but increase to > 10 dB at lower frequencies in most conditions.

Analysis across the population of specimens is shown in Figure 3. Figure 3A shows the mean (± SEM; light gray bands) transfer functions (H_{Stap}, H_{SV}, and H_{ST}) recorded under baseline (circles) and electrode inserted conditions (symbols) across the population of specimens. Transfer functions are shown superimposed over the range of responses observed in normal responses reported in the literature (dark gray bands) (23,35). As in the individual example shown above, the population means show substantial overlap across the range of frequencies tested. The only condition in which a change from baseline appears present is at moderate frequencies in ST, though overlap between conditions in substantial. Responses show sharp increases at the highest and lowest frequencies in some conditions, which likely result from low signal strength in those recordings. Transfer function phase was similarly compared across electrode conditions (not shown). No substantial differences are noted with respect to baseline, or across electrode conditions.

In order to facilitate comparisons across conditions, Figure 3B shows the mean (± SEM) differences between electrode conditions and baseline across all specimens tested. Differences are calculated with respect to baseline for each specimen, and thus are shown only when at least two specimens were recorded with signal-to-noise ratios greater than 3 dB in both the baseline and experimental conditions, thus comparisons are shown for fewer frequencies than in Figure 3A. H_{Stap} decreased by a small amount (<5 dB) with respect to control at most frequencies, suggesting that the cochlear input impedance may have increased somewhat (23). Similarly, H_{SV} was essentially unchanged from control for all frequencies, while H_{ST} was increased somewhat compared to control at low to moderate frequencies in most electrode conditions, suggesting a somewhat decreased differential intracochlear pressure.

Quantitative comparisons of transfer function changes during electrode conditions compared to control are summarized in Figure 4. Responses were grouped into three frequency bands with relatively low ($f < 1$ kHz), middle (1 kHz < f < 3 kHz), and high ($f > 3$ kHz) frequencies, and roughly the same number of frequencies (~3) within each band. A two-way analysis of variance was performed with *response gain re baseline* as the dependent, and electrode insertion and frequency bands as independent variables. Results for H_{Stap} and H_{SV} reveal no significant main effects of electrode insertion ($F_{6,390/290} = 1.05$ & 1.29; $p = 0.39$ & 0.26, respectively), or frequency band ($F_{2,390/290} = 0.18$ & 1.45; $p = 0.83$ & 0.24, respectively), with no significant interaction ($F_{12,390/290} = 0.27$ & 0.15; $p > 0.99$ & 0.99, respectively). Conversely, significant main effect were observed in H_{ST} for both frequency ($F_{2,229} = 19.15$; $p \ll 0.001$) and electrode insertion ($F_{6,229} = 3.06$; $p = 0.031$), with no significant interaction ($F_{12,229} = 1.14$; $p = 0.32$). Post-hoc Tukey HSD pairwise comparisons

reveal that the highest frequency band is significantly different from both the low and middle bands in H_{ST} ($p \ll 0.001$), which were not significantly different from each other, and baseline was significantly different from the NCA ($p = 0.042$), while other pairs were not ($p > 0.1$).

Effect of CI electrode insertion on differential intracochlear pressure

The significant increases in H_{ST} in the low and moderate frequency bands, without a commensurate increase in H_{SV} indicates that the differential intracochlear sound pressure, which drives the motion of the cochlear partition, has changed following cochlear implant electrode insertion. In order to assess this change directly, Figure 5 shows directly the mean (±SEM) differential pressure normalized to the sound pressure level in the ear canal, defined as $(P_{SV} - P_{ST})/P_{EC}$. Differential intracochlear pressure is greatest in the baseline condition at all frequencies. The effect of cochlear implant electrode insertion was a decrease in differential pressure of ~5 dB at moderate sound pressure levels. Significance of this change was assessed with a two-way analysis of variance, performed with *response gain re baseline* as the dependent, and electrode insertion and frequency bands as independent variables. Main effects of both condition ($F_{6,22} = 2.46$, $p = 0.025$) and frequency ($F_{2,222} = 23.9$, $p \ll 0.001$) are evident, with no significant interaction ($F_{12,222} = 0.55$, $p = 0.883$). Post-hoc Tukey HSD pairwise comparisons reveal that the baseline condition is significantly different from MS, NCA, and 1J conditions ($p < 0.05$), nearly significantly different from the HL24 and SS25 conditions ($p < 0.1$), and not different from the SS20 condition ($p = 0.235$). All three frequency bands are significantly different from one another ($p < 0.05$), and particularly the low frequency band from the moderate and high frequency bands ($p \ll 0.001$).

Discussion

Hearing preservation following CI implantation has become a topic of great interest in patients undergoing cochlear implantation. EAS has shown benefits in music appreciation, sound localization, and improved speech perception, especially in noise (2–4), thus significant effort has been dedicated to improvements in both electrode design and surgical technique. Despite recent technological advancements, a significant increase in audiometric thresholds is common postoperatively (37–39).

Loss of residual hearing with CI insertion was historically thought to be primarily due to damage to neural elements within the cochlea, however, recent data indicates a certain percentage of these losses may be conductive in nature (10–13). The incidence of this loss may also be underestimated due to limitations with bone-conduction audiometry such as vibrotactile responses and masking dilemmas, especially in those with severe to profound hearing loss (10,14).

Proposed mechanisms for conductive losses following CI insertion include changes in middle ear (e.g. effusion) or inner ear mechanics, damage to intracochlear structures (e.g. basilar membrane, osseous spiral lamina, spiral ligament), change in perilymph volume, alteration of RW compliance, and inflammatory reactions surrounding the electrode itself (e.g. fibrosis, osteoneogenesis) (10,11,14–17). At this point, however, the etiology is

unclear. In this manuscript we explored the effects of several common, commercially available CI electrode designs on middle and inner ear mechanics to evaluate if the presence of a CI electrode could be responsible for these changes.

Our results indicate a minimal effect on V_{Stap} and only small effects on P_{IC} following CI electrode insertion. In general, a small increase in P_{ST} and not in P_{SV}, likely as a result of the presence of the CI electrode in the scala tympani, results in a decrease to the differential intracochlear pressure, a direct measure of the drive provided to the cochlear partition, of only ~5 dB. This decrease is insufficient to explain the substantial decrease in residual hearing observed in some patients, but could contribute to any conductive loss observed. These effects were consistent across several different electrodes produced by different manufacturers, suggesting a consistent mechanism underlies these small response changes despite differences in electrode design and geometry.

Various studies have been contradictory regarding the influence of a CI electrode on the mechanics on the middle and inner ears. Donnelly et al. showed significant variability in the effect of cochlear implantation on V_{Stap} as measured by LDV *in vivo*, though these changes were thought to be due to operative variability, specifically the amount of perilymph lost with cochleostomy and insertion of the electrode (17). Prior studies support this theory, showing differences in static displacement of the ossicles, vibratory velocity, and vibratory amplitude with changes in intracochlear pressures (18–21). These studies demonstrated that vibratory amplitude and stapes displacement is inversely proportional to amount of cochlear fluid (19–22).

Our results are consistent with prior reports concluding a minimal effect on middle and inner ear mechanics with a CI electrode in place. Kiefer et al., using a finite element analysis model, showed alterations in basilar membrane displacement at the apical and basal ends of a CI electrode due to stiffening of the basilar membrane (15). However, this seemed to only occur in mid to high-frequency acoustic signals and actually resulted in increased displacement adjacent to these areas, while predicting little impact on low frequency acoustic perception (15). Pazen et al. presented preliminary results suggesting that a CI electrode minimally affects the magnitude of stapes and round window velocity, independent of electrode insertion path or electrode geometry (40). Additionally, Huber et al. showed minimal change (<3 dB) in RW or stapes vibrational behavior before and after electrode insertion *in vivo* (16). Based upon their results and the small cross-sectional area of the electrode used, they determined that the introduction of a CI electrode does not alter the mechanics of cochlear fluid to the point of clinical relevance (16).

There is also concern of potential host responses toward the electrode itself resulting in fibrosis or osteoneogenesis. Mechanisms behind this hearing loss include both inflammatory and mechanical theories, with the latter resulting in alteration of passive cochlear mechanics and possible conductive hearing losses (41–43). Choi and Oghalai (42) used a mathematical model of passive cochlear mechanics to show damping (i.e., caused by fibrosis) of the ST predicted an elevation of low-frequency hearing thresholds. Other studies have also shown these reactions may be focused at specific regions within the cochlea, and although the usual location was close to the basal turn near the RW, it may also extend apically toward low

frequency areas of the cochlea (44–47). These reactions could certainly alter the mechanics of the inner ear by increasing damping of the cochlear partition, or altering compliance of the RW and motion of the stapes (10,14,41–43). Raveh et al. discussed the possibility that these inner ear changes could affect air conduction more so than bone conduction, resulting in an air-bone gap (14). However, the contribution of this mechanism is unclear, as our methodology cannot mimic these changes.

Conclusion

Hearing preservation is of the utmost importance in those undergoing cochlear implantation, especially as guidelines change to include those with more residual hearing. Significant effort has been placed upon improving both surgical technique and electrode design to limit loss of residual hearing when possible. Our results indicate that this effort has been worthwhile, and suggest that continued improvement of electrode design and surgical technique will help minimize further loss of residual hearing, both sensorineural and conductive in nature (10). The etiology of conductive losses continues to be unknown, but our results indicate altered middle and inner ear mechanics due to a CI electrode contribute minimally (~5 dB), even across multiple electrodes with varying lengths and configurations. Therefore, we suspect loss of residual hearing, specifically due to a conductive component, is likely indirect or a combination of different mechanisms.

Additionally, we feel it is important to measure both air and bone conduction thresholds during audiometry (and possibly tympanometry) post-operatively to assess for possible unrecognized conductive components that could be contributing to increases in threshold (10). However, this may be difficult to assess in lower frequencies due to limitations of bone conduction audiometry, and as a result, the presence of conductive losses may be underestimated in those with significant hearing loss. Thus, we cannot over emphasize the importance of considering a conductive loss in those with increased thresholds post-operatively (10).

Acknowledgments

Funding:

Funding was provided by NIH/NIDCD: 1T32-DC012280 (NTG).

Funding was provided by NIH/NIDCD T32 DC012280 (NTG). We appreciate the assistance of Dr. Michael Hall in constructing some of the custom experimental equipment (support by NIH grant P30 NS041854).

References

1. Clark GM. The multi-channel cochlear implant: Multi-disciplinary development of electrical stimulation of the cochlea and the resulting clinical benefit. Hear Res. 2014
2. Gantz BJ, Turner CW. Combining acoustic and electrical hearing. Laryngoscope. 2003; 113:1726–30. [PubMed: 14520097]
3. von Ilberg C, Kiefer J, Tillein J, et al. Electric-acoustic stimulation of the auditory system. New technology for severe hearing loss. ORL J Otorhinolaryngol Relat Spec. 1999; 61:334–40. [PubMed: 10545807]
4. Turner CW, Gantz BJ, Vidal C, et al. Speech recognition in noise for cochlear implant listeners: benefits of residual acoustic hearing. J Acoust Soc Am. 2004; 115:1729–35. [PubMed: 15101651]

5. Balkany TJ, Connell SS, Hodges AV, et al. Conservation of residual acoustic hearing after cochlear implantation. Otology & Neurotology. 2006; 27:1083–8. [PubMed: 17130798]
6. Adunka O, Kiefer J, Unkelbach MH, et al. Development and evaluation of an improved cochlear implant electrode design for electric acoustic stimulation. The Laryngoscope. 2004; 114:1237–41. [PubMed: 15235353]
7. Adunka O, Kiefer J. Impact of electrode insertion depth on intracochlear trauma. Otolaryngol Head Neck Surg. 2006; 135:374–82. [PubMed: 16949967]
8. James C, Albegger K, Battmer R, et al. Preservation of residual hearing with cochlear implantation: how and why. Acta Otolaryngol. 2005; 125:481–91. [PubMed: 16092537]
9. Eshraghi AA. Prevention of cochlear implant electrode damage. Current opinion in otolaryngology & head and neck surgery. 2006; 14:323–8. [PubMed: 16974145]
10. Chole RA, Hullar TE, Potts LG. Conductive component after cochlear implantation in patients with residual hearing conservation. Am J Audiol. 2014; 23:359–64. [PubMed: 25165991]
11. Lenarz T, Stover T, Buechner A, et al. Temporal bone results and hearing preservation with a new straight electrode. Audiol Neurootol. 2006; 11 (Suppl 1):34–41. [PubMed: 17063009]
12. Tamir S, Ferrary E, Borel S, et al. Hearing preservation after cochlear implantation using deeply inserted flex atraumatic electrode arrays. Audiol Neurootol. 2012; 17:331–7. [PubMed: 22813984]
13. Usami S, Moteki H, Suzuki N, et al. Achievement of hearing preservation in the presence of an electrode covering the residual hearing region. Acta Otolaryngol. 2011; 131:405–12. [PubMed: 21208024]
14. Raveh E, Attias J, Nageris B, et al. Pattern of hearing loss following cochlear implantation. European Archives of Oto-Rhino-Laryngology. 2014:1–6.
15. Kiefer J, Bohnke F, Adunka O, et al. Representation of acoustic signals in the human cochlea in presence of a cochlear implant electrode. Hear Res. 2006; 221:36–43. [PubMed: 16962268]
16. Huber AM, Hoon SJ, Sharouz B, et al. The influence of a cochlear implant electrode on the mechanical function of the inner ear. Otol Neurotol. 2010; 31:512–8. [PubMed: 20061991]
17. Donnelly N, Bibas A, Jiang D, et al. Effect of cochlear implant electrode insertion on middle-ear function as measured by intra-operative laser Doppler vibrometry. J Laryngol Otol. 2009; 123:723–9. [PubMed: 19138455]
18. Murakami S, Gyo K, Goode RL. Effect of increased inner ear pressure on middle ear mechanics. Otolaryngol Head Neck Surg. 1998; 118:703–8. [PubMed: 9591878]
19. Gundersen T, Hogmoen K. Holographic vibration analysis of the ossicular chain. Acta Otolaryngol. 1976; 82:16–25. [PubMed: 948981]
20. Gyo K, Aritomo H, Goode RL. Measurement of the ossicular vibration ratio in human temporal bones by use of a video measuring system. Acta Otolaryngol. 1987; 103:87–95. [PubMed: 3564932]
21. Gan RZ, Sun Q, Dyer RK Jr, et al. Three-dimensional modeling of middle ear biomechanics and its applications. Otol Neurotol. 2002; 23:271–80. [PubMed: 11981381]
22. Lord RM, Abel EW, Wang Z, et al. Effects of draining cochlear fluids on stapes displacement in human middle-ear models. J Acoust Soc Am. 2001; 110:3132–9. [PubMed: 11785814]
23. Nakajima HH, Dong W, Olson ES, et al. Differential intracochlear sound pressure measurements in normal human temporal bones. J Assoc Res Otolaryngol. 2009; 10:23–36. [PubMed: 19067078]
24. Olson ES. Observing middle and inner ear mechanics with novel intracochlear pressure sensors. J Acoust Soc Am. 1998; 103:3445–63. [PubMed: 9637031]
25. Olson ES. Direct measurement of intra-cochlear pressure waves. Nature. 1999; 402:526–9. [PubMed: 10591211]
26. Greene, NT.; Mattingly, JK.; Jenkins, HA., et al. Some Investigations into the mechanisms of bone conducted sound. 38th Annual MidWinter Meeting of the Association for Research in Otolaryngology; 2015.
27. Mattingly, JK.; Greene, NT.; Jenkins, HA., et al. Effects of Ipsilateral and contralateral placement of bone-conduction systems on cochlear input signal. 38th Annual MidWinter Meeting of the Association for Research in Otolaryngology; 2015.

28. Tringali S, Koka K, Jenkins HA, et al. Sound Location Modulation of Electrocochleographic Responses in Chinchilla With Single-Sided Deafness and Fitted With an Osseointegrated Bone-Conducting Hearing Prosthesis. Otology & neurotology: official publication of the American Otological Society, American Neurotology Society [and] European Academy of Otology and Neurotology. 2014
29. Tringali S, Koka K, Deveze A, et al. Round window membrane implantation with an active middle ear implant: a study of the effects on the performance of round window exposure and transducer tip diameter in human cadaveric temporal bones. Audiol Neurootol. 2010; 15:291–302. [PubMed: 20150727]
30. Deveze A, Koka K, Tringali S, et al. Active middle ear implant application in case of stapes fixation: a temporal bone study. Otol Neurotol. 2010; 31:1027–34. [PubMed: 20679957]
31. Lupo JE, Koka K, Jenkins HA, et al. Vibromechanical Assessment of Active Middle Ear Implant Stimulation in Simulated Middle Ear Effusion: A Temporal Bone Study. Otology & Neurotology. 2014; 35:470–5. [PubMed: 23988990]
32. Stenfelt S, Hato N, Goode RL. Round window membrane motion with air conduction and bone conduction stimulation. Hear Res. 2004; 198:10–24. [PubMed: 15567598]
33. Stenfelt S, Hato N, Goode RL. Fluid volume displacement at the oval and round windows with air and bone conduction stimulation. J Acoust Soc Am. 2004; 115:797–812. [PubMed: 15000191]
34. ASTM. ASTM Standard F2504-05(2014). West Conshohocken, PA: 2014. Standard Practice for Describing System Output of Implantable Middle Ear Hearing Devices.
35. Rosowski JJ, Chien W, Ravicz ME, et al. Testing a method for quantifying the output of implantable middle ear hearing devices. Audiol Neurootol. 2007; 12:265–76. [PubMed: 17406105]
36. Deveze A, Koka K, Tringali S, et al. Techniques to improve the efficiency of a middle ear implant: effect of different methods of coupling to the ossicular chain. Otol Neurotol. 2013; 34:158–66. [PubMed: 23196747]
37. Brown RF, Hullar TE, Cadieux JH, et al. Residual hearing preservation after pediatric cochlear implantation. Otol Neurotol. 2010; 31:1221–6. [PubMed: 20818293]
38. Friedland DR, Runge-Samuelson C. Soft cochlear implantation: rationale for the surgical approach. Trends in amplification. 2009; 13:124–38. [PubMed: 19447766]
39. Lenarz T, James C, Cuda D, et al. European multi-centre study of the Nucleus Hybrid L24 cochlear implant. Int J Audiol. 2013; 52:838–48. [PubMed: 23992489]
40. Pazen, D.; Nunning, M.; Anagiotos, A., et al. The impact of a cochlear implant electrode array on middle ear transfer function: a temporal bone study. 13th International Conference on Cochlear Implants and Other Implantable Auditory Technologies; Munich, Germany. 2014.
41. O'Leary SJ, Monksfield P, Kel G, et al. Relations between cochlear histopathology and hearing loss in experimental cochlear implantation. Hear Res. 2013; 298:27–35. [PubMed: 23396095]
42. Choi CH, Oghalai JS. Predicting the effect of post-implant cochlear fibrosis on residual hearing. Hear Res. 2005; 205:193–200. [PubMed: 15953528]
43. Eshraghi AA, Polak M, He J, et al. Pattern of hearing loss in a rat model of cochlear implantation trauma. Otol Neurotol. 2005; 26:442–7. discussion 7. [PubMed: 15891647]
44. Nadol JB Jr, Eddington DK. Histologic evaluation of the tissue seal and biologic response around cochlear implant electrodes in the human. Otol Neurotol. 2004; 25:257–62. [PubMed: 15129102]
45. Li PM, Somdas MA, Eddington DK, et al. Analysis of intracochlear new bone and fibrous tissue formation in human subjects with cochlear implants. Ann Otol Rhinol Laryngol. 2007; 116:731–8. [PubMed: 17987778]
46. Somdas MA, Li PM, Whiten DM, et al. Quantitative evaluation of new bone and fibrous tissue in the cochlea following cochlear implantation in the human. Audiol Neurootol. 2007; 12:277–84. [PubMed: 17536196]
47. Seyyedi M, Nadol JB Jr. Intracochlear inflammatory response to cochlear implant electrodes in humans. Otol Neurotol. 2014; 35:1545–51. [PubMed: 25122600]

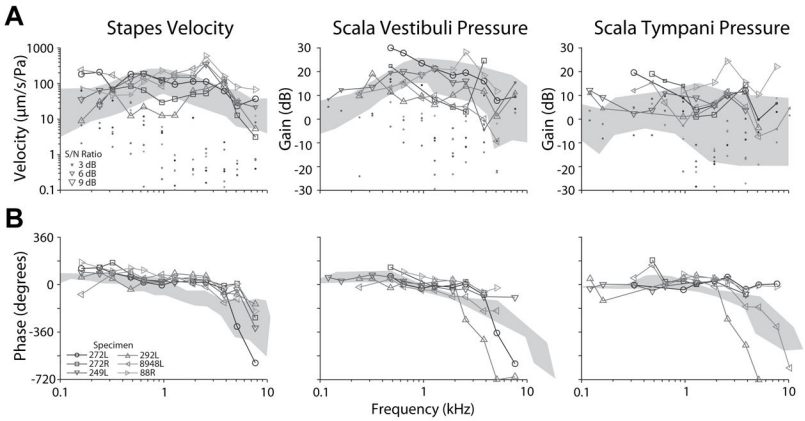

Figure 1.

Baseline stapes velocity (V_{Stap}), and scala vestibuli and tympani pressure ($P_{SV/ST}$) transfer function magnitudes **(A)** and phases **(B)**. Responses recorded in the six specimens meeting inclusion criteria are shown normalized to the sound pressure level recorded in the ear canal. Responses are superimposed onto the 95% CI and range of responses (gray areas) observed previously in V_{Stap} and $P_{SV/ST}$, respectively (23,35). Symbol size in **(A)** indicates the signal to noise ratio (small: > 3 dB, medium: > 6 dB, large: > 9 dB), and dots show the noise floor for each measurement (normalized as: noise/P_{EC} during sound stimulation).

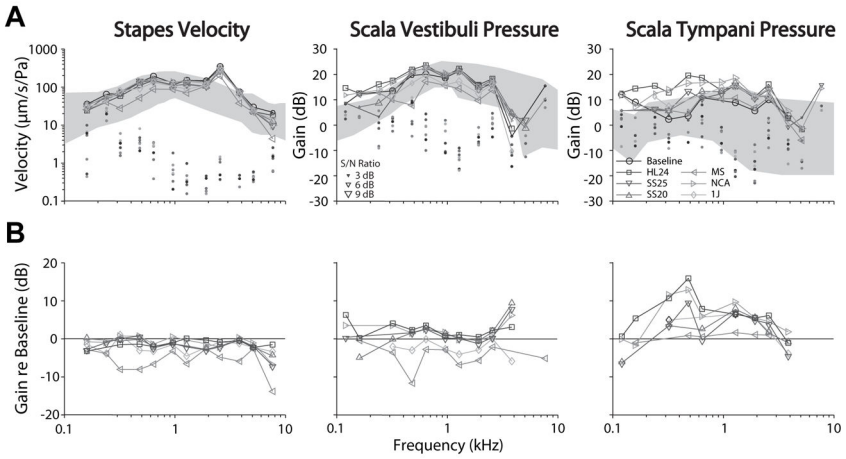

Figure 2.

An example set of recordings in one representative specimen (249L). **(A.)** Baseline transfer functions are represented by circles, while transfer functions recorded with various CI electrodes shown in the legend. **(B.)** Difference in transfer function magnitude recorded with each CI electrode inserted compared to the baseline for the same specimen as in **(A.)**. Responses are shown in units of dB difference from baseline as a function of stimulus frequency. Symbol size indicates the signal to noise ratio (small: > 3 dB, medium: > 6 dB, large: > 9 dB), and dots show the noise floor for each measurement (normalized as: noise/P_{EC} during sound stimulation). Nucleus Hybrid L24 (HL24), Nucleus CI422 Slim Straight inserted at 20 and 25 mm (SS20 & SS25), Nucleus CI24RE Contour Advance (NCA), HiFocus Mid-Scala (MS), and HiFocus 1j (1j).

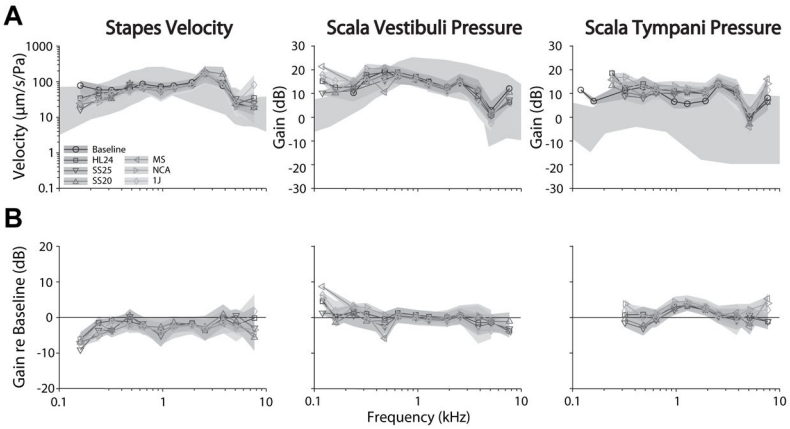

Figure 3.

Analysis of the responses across the population of specimens is shown. **(A.)** The mean (± SEM; gray bands) transfer functions across specimens, recorded under baseline (circles) and CI electrode inserted conditions (symbols) for V_{Stap} (left), P_{SV} (center) and P_{ST} (right) magnitudes. Responses are shown superimposed over the same range of responses shown in prior reports (dark gray bands) (23,35). **(B)** The mean (± SEM) differences (in dB re: baseline) compared to baseline across all specimens tested. Nucleus Hybrid L24 (HL24), Nucleus CI422 Slim Straight inserted at 20 and 25 mm (SS20 & SS25), Nucleus CI24RE Contour Advance (NCA), HiFocus Mid-Scala (MS), and HiFocus 1j (1j).

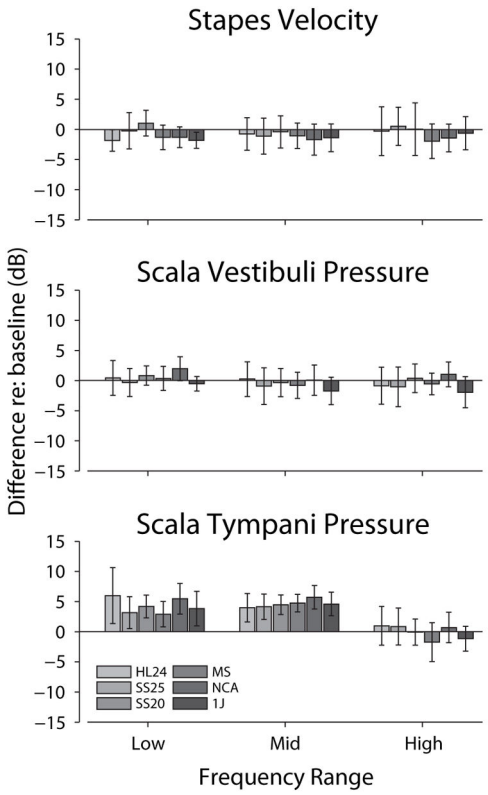

Figure 4.

Summary of the effects of inserting different cochlear implant electrodes into the ST with respect to the acoustic baseline. Responses were grouped within three frequency bands with relatively low (f < 1 kHz), middle (1 kHz < f < 3 kHz), and high (f > 3 kHz) frequencies. Responses are shown as the average difference within each frequency band, for each electrode condition. See the RESULTS for a description of the statistical analysis. Nucleus Hybrid L24 (HL24), Nucleus CI422 Slim Straight inserted at 20 and 25 mm (SS20 & SS25), Nucleus CI24RE Contour Advance (NCA), HiFocus Mid-Scala (MS), and HiFocus 1j (1j).

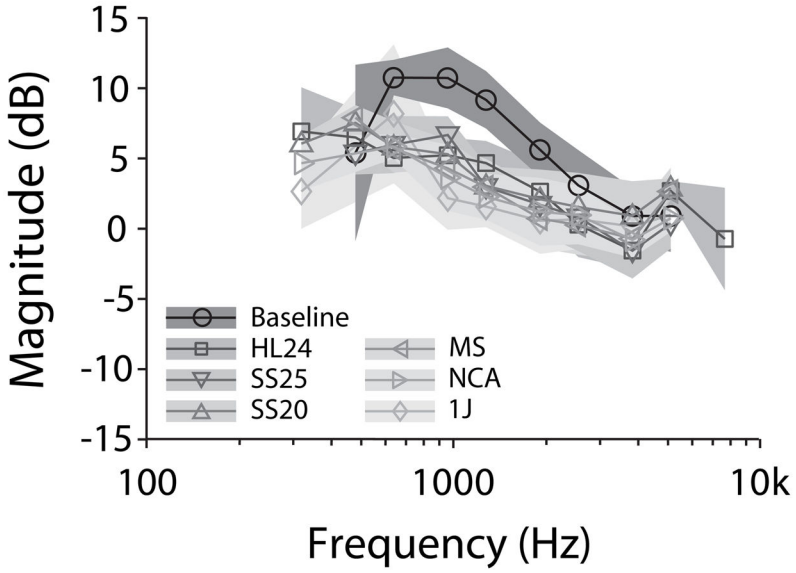

Figure 5.

Mean (±SEM) effects of inserting the cochlear implant electrodes into the ST on differential intracochlear pressure, $(P_{SV}-P_{ST})/P_{EAC}$. Nucleus Hybrid L24 (HL24), Nucleus CI422 Slim Straight inserted at 20 and 25 mm (SS20 & SS25), Nucleus CI24RE Contour Advance (NCA), HiFocus Mid-Scala (MS), and HiFocus 1j (1j).

Table 1

Dimensions (mm) of the CI electrodes used in the study: Nucleus Hybrid L24, Nucleus CI422 Slim Straight 20 and 25 mm, Nucleus CI24RE Contour Advance, HiFocus Mid-Scala, and HiFocus 1j.

Implant	Electrode Length	Basal diameter	Apical diameter	Tip diameter
Cochlear Nucleus Hybrid L24	16	0.4	0.25	n/a
Cochlear Nucleus Slim Straight CI422	20 and 25	0.6	0.3	n/a
AB HiFocus Mid- scala	18.5	0.7	0.5	n/a
Cochlear Nucleus CI24RE Contour advance	20	0.8	0.5	0.2
AB HiFocus 1J	25	0.8	0.4	n/a